# Effects of ionospheric plasma irregularities at the equatorial zone on GPS signal

Amath Ndao, Idrissa Gaye, Rolland Fleury, Cheikh Sarr, Christine Amory Mazaudier

# Effects of ionospheric plasma irregularities at the equatorial zone on GPS signal.

**[1]Amath NDAO, [1]Idrissa GAYE*, [2]Rolland Fleury, [1]Cheikh SARR, [3]Christine Amory Mazaudier,**

1. University Iba Der THIAM of Thiès (UIDT) - Senegal

2. Institut Mines-Telecom Brest – France

3. LPP UPMC Paris – France

Email correspondence Author: idrissa.gaye@univ-thies.sn

This paper studies scintillations of the GPS signal in the equatorial zone created by the ionospheric plasma irregularities.

RINEX Data resulting from GPS stations located at ±20° from the magnetic equator were used.

This study was carried out by considering three GPS stations including the station from Dakar, that of Yamoussoukro and that of Cotonou. They belong to the IGS (International GNSS Services) network.

The equatorial zone is one of most impacted areas by ionospheric irregularities causing scintillations of GPS signal which affect the phase measurement and thus can degrade the GPS receiver's performances during a positioning. The ROTI index was calculated to detect existing ionospheric irregularities.

This index enabled us to detect scintillations of the GPS signal on a positioning situation.

**Keywords:** Ionospheric irregularities; Scintillation; Equatorial zone; TEC; ROTI; GPS; Positioning.

## 1. Introduction

The first objective of GPS was a military use for positioning. The GPS system was set up since 1973 with 24 satellites. It turns out that the signal emitted by the satellite which crosses the layers of the atmosphere is disturbed and therefore this has made it possible to develop science research. So the use for space weather came later **[1]**.

Nowadays, the Global Positioning System (GPS) is used by many applications for positioning services. This system is currently made up of 32 satellites around the earth at an altitude of 20200 km. Its goal is to provide location, anywhere on the planet, anytime and regardless of weather conditions, with accurate positioning, navigation and timing (PNT).

The ionosphere is an ionized part of atmosphere and extends between 70 and 1000 km above sea level. It is a plasma made up of neutral molecules and ionized particles. Ionization is caused by solar X-ray and UV radiation **[2]**. Crossing the ionosphere delays the propagation time and advances the phase measurement. The disturbance intensity is proportional to the total electronic content (TEC). It is the first cause in the positioning degradation. The main parameter that characterizes the ionosphere is the vertical profile, the ionospheric ionization and the total electronic content (TEC). The most significant variations in electron density are found at high latitudes and in the equatorial zone of the ionosphere **[3],[4].** These depend on the local time, seasons and solar activity.

At sunset at the equator (low latitudes), the electric current in region E (100 km) and the electric field directed towards the East during the day increases quicly before heading towards the West this is

called the PRE Pre Reversal Enhancement, this fast increase in the electric field associated with a decrease ionization causes a Rayleigh Taylor instability causing plasma bubbles at the equator **[5].**

Crossing of ionospheric irregularities by the GNSS signal causes its diffusion which will result in quick amplitude and phase fluctuations at the receiver level. The morphology of equatorial scintillations of the GPS signal is characterized by the 11-year sunspot cycle, seasonal or annual dependence, and spatial distribution. The spatial distribution is dominated by the highest ionospheric electron densities location, which are the anomalies, about 15 degrees from the magnetic equator **[6]**

In this work, two distinct moments are considered: a moment without scintillation and another with scintillation. Data are for the year 2015 characterized by average solar activity (R12 between 40 and 65). These data allow us to calculate both, the ROTI index and the VTEC variation and come from three stations located in the equatorial zone ± 20 ° from the magnetic equator. These locations are Dakar, Yamoussoukro and Cotonou stations which are in the IGS network **[7]**

We first do a theoretical study of density gradients in the ionosphere, then we will present our methodology and approach to study this phenomenon and its impact on positioning by GPS and finally the last part will be devoted to results and discussions.

## 2. Morphology of ionosphéric irregularities.

Ionospheric irregularities is a phenomenon that affect radio waves through the ionosphere by quick fluctuation of their amplitude and phase. It is frequently observed at peak solar activity and in equatorial and auroral regions. As indicated previously, it affects GPS signals and thus reduces the positioning measurements accuracy.

Many authors have studied this phenomenon, but like all natural phenomena, it is very difficult to predict large-scale ionospheric irregularities. It is caused by under-ionized irregularities in electron density gradient. Most ionospheric irregularities occur during the several hours after sunset (8 p.m.-2 a.m. TL) during solar maximum **[8], [9], [10], [11]**.

The ionospheric irregularities can be quantified using the S4 amplitude scintillation index, and the phase scintillation index $\boldsymbol{\sigma_{\varphi}}$.

### 2.1. Amplitude an phase scintillation index

- Amplitude scintillation is quantified by the S4 index which is defined as the normalized standard deviation of the received signal intensity I over a given time interval and is expressed by the following relationship **[3]:**

$$S_4 = \frac{\sqrt{\langle I^2 \rangle - \langle I \rangle^2}}{\langle I \rangle} \qquad (1)$$

Where $\langle I \rangle$ is the time average of I.

- Phase scintillation is measured by $\sigma_\varphi$ index which is defined as the normalized standard deviation of the phase signal over a given time interval and is expressed as **[12]**

$$\sigma_\varphi = \sqrt{\langle \varphi^2 \rangle - \langle \varphi \rangle^2} \qquad (2)$$

### 2.2. ROTI index

Another method of approaching ionospheric irregularities is based on ROTI index calculation used to characterize plasma bubbles **[7], [13], [14]**. The Slant Total Electronic Content (STEC) is calculated from the two phase measurements (L1 and L2) recorded by the dual-frequency geodetic receivers and archived in RINEX format. Strong phase jumps are detected and corrected on the time series. One then calculates the temporal gradient at the two instants k and (t + Δt).

The ROT (Rate of the TEC), expressed in tecu / min, is calculated by the following relationship **[13]**.

$$ROT = \frac{STEC_{t+\Delta t} - STEC_t}{time_{t+\Delta t} - time_t} \qquad (3)$$

Where STEC represents the total relative oblique electronic content calculated from the phase measurements L1 and L2 on the two frequencies f1 (1575.42 MHz) and f2 (1227.60 MHz). The STEC is given by the relation:

$$STEC = \frac{1}{40.3}\left[\frac{f_1^2 f_2^2}{f_1^2 - f_2^2}\right](L_2 - L_1) \qquad (4)$$

From the ROT value calculated over each 30s interval, we calculate the ROTI index: This is the standard deviation of the ROT values over a time interval chosen at 5 minutes.

$$ROTI = \sqrt{\langle ROT^2 \rangle - \langle ROT \rangle^2} \qquad (5)$$

The index characterizes small-scale and / or rapid variation in total electronic content and is strongly related to scintillation **[16], [17].**

The variation range of the ROTI index on the ordinate is between 0 and 6 tecu / mn. The zone between 0 and 1 can be likened to noise. Above the value 1, it can be said that scintillation is present. We are in very strong scintillation conditions above about 2.5 tecu / mn.

## 3. Methodology and approach

In this work, we used the RINEX files from the Dakar, Yamoussoukro and Cotonou GPS stations, for modeling VTEC and ROTI index variations. We have targeted these three stations which are located at ± 20° from the magnetic equator, therefore closer to the equatorial zone. The following Table1 gives geographical positioning of tree (03) treated GPS stations located at ± 20° from the magnetic equator.

Table 1: Geographical position of the treated GPS stations located at ± 20° from the magnetic equator.

| GPS marker | Latitude | Longitude |
|---|---|---|
| BJCO | 6.985°N | 2.450°E |
| DAKR | 14.721°N | -17.440°E |
| YKRO | 6.871°N | -5.240°E |

The dynamic positioning is obtained by the RTKlib software, which is a library of free open source softwares, portable and composed of several access points for processing GNSS data **[18]**.

To study ionospheric irregularities, two particular periods of the year 2015 are chosen according to the level of solar activity. We consider one day of March 2015 and one day of July 2015 which are respectively periods of high and low solar activity.

VTEC and ROTI index calculation are carried out by Matlab software developed by GIRGEA team, from R. Fleury. It is available on the GIRGEA website (www.girgea.com).

## 4. Results et discussions

### 4.1. VTEC analysis

Before analyzing our results over the 2 selected days, we study the spatial VTEC variation across the globe. These variations are provided by GIM / CODG maps in IONEX format using software provided by Leica **[19]**

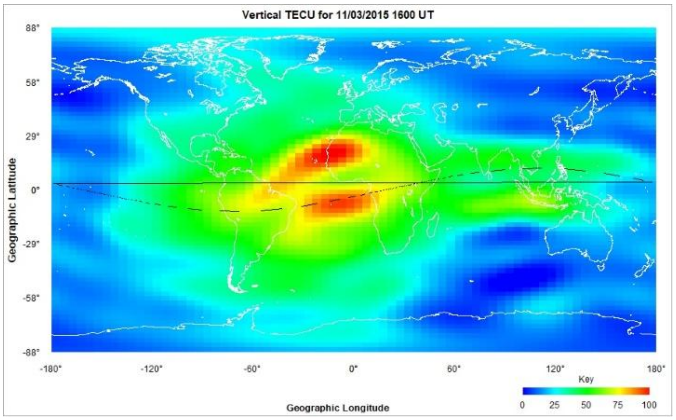


***Figure 1a :*** *Distribution of VTEC on March 11th, 2015 at 4 p.m. UT*

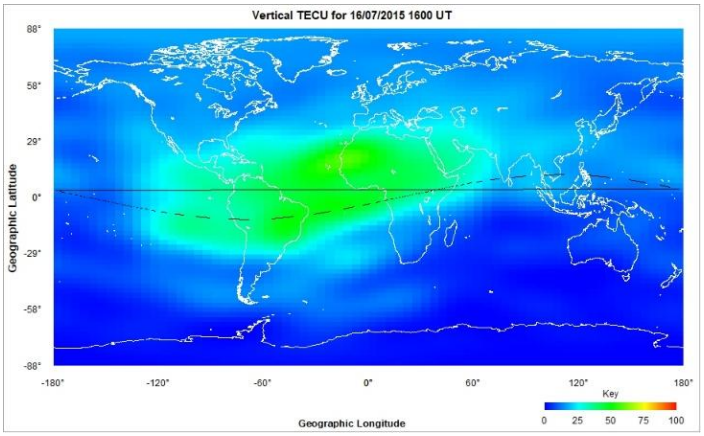


***Figure 1b:*** *Distribution of VTEC on July 16th 2015 at 4 p.m. UT*

Figure 1a and Figure 1b shows the spatial variation of the VTEC on March 11th 2015 and July 16th 2015 at 4 p.m. universal time with geographic longitude on the x-axis and longitude on the y-axis. In the first case, we visually see two strong north and south ridges, red in color associated with values greater than 90 tecu and centered on the 14-16 TL time slot: this is the crests of the equatorial anomaly. The maxima are on either side of the magnetic equator. The anomaly continues with still strong levels (~ 50 tecu) up to longitude 150 ° E or two local hours. It then disappears in the last hours of the night. For the second figure, we kept the same scale of the VTEC. The two red zones have disappeared, giving way to a yellow zone, ie values around 50 tecu. The area in green color (40 tecu) is much smaller than in the previous case. This result is consistent with the seasonal variation with a maximum VTEC on the 2 equinoxes and minimum in summer. The dark blue area is larger in the southern hemisphere (winter, almost permanent night) than in the northern hemisphere (permanent day) **[20], [21], [22]**.

To illustrate the results of this work, we have plotted in Figures 2a, 2b, 3a, 3b, 4a and 4b the variations of the VTEC as a function of time (TU).

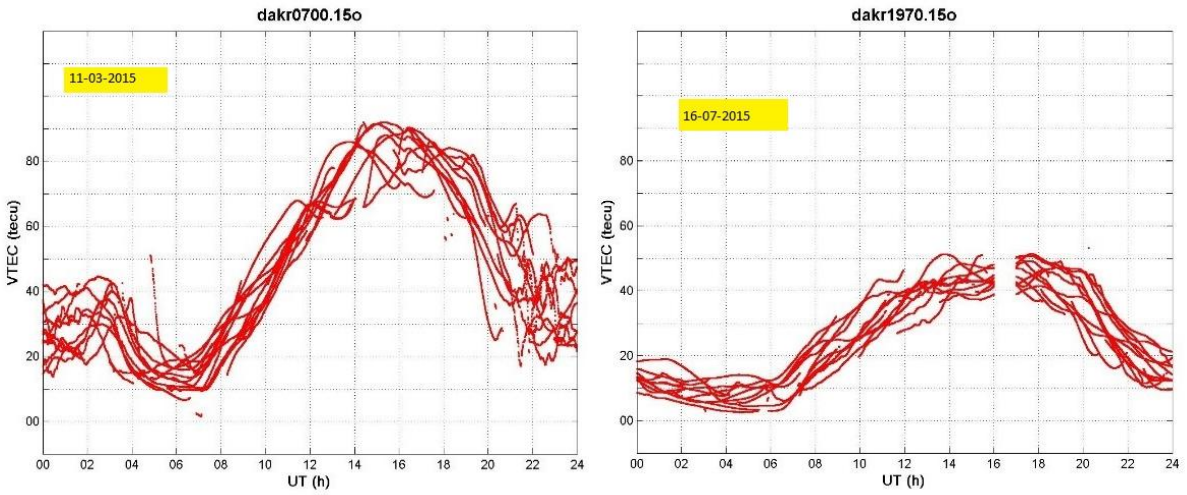

***Figure 2a*** ***Figure 2b***

*Plots of VTEC variation respectively for March 11th 2015 and July 16th 2015 of the Dakar station (DAKR)*

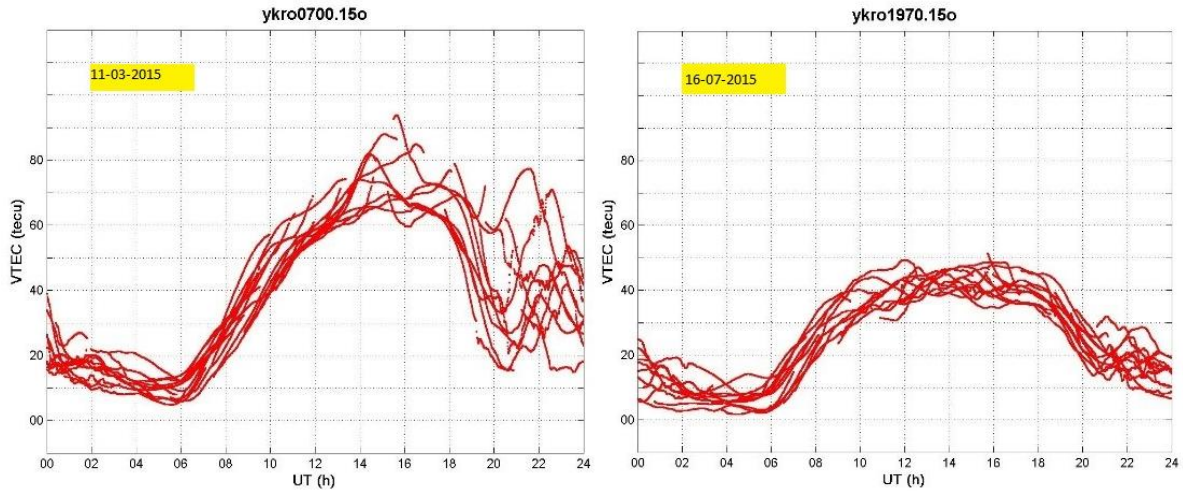


***Figure 3a*** ***Figure 3b***

*Plots of VTEC variation respectively for March 11th 2015 and July 16th 2015 of the Yamoussoukro station (YKRO)*

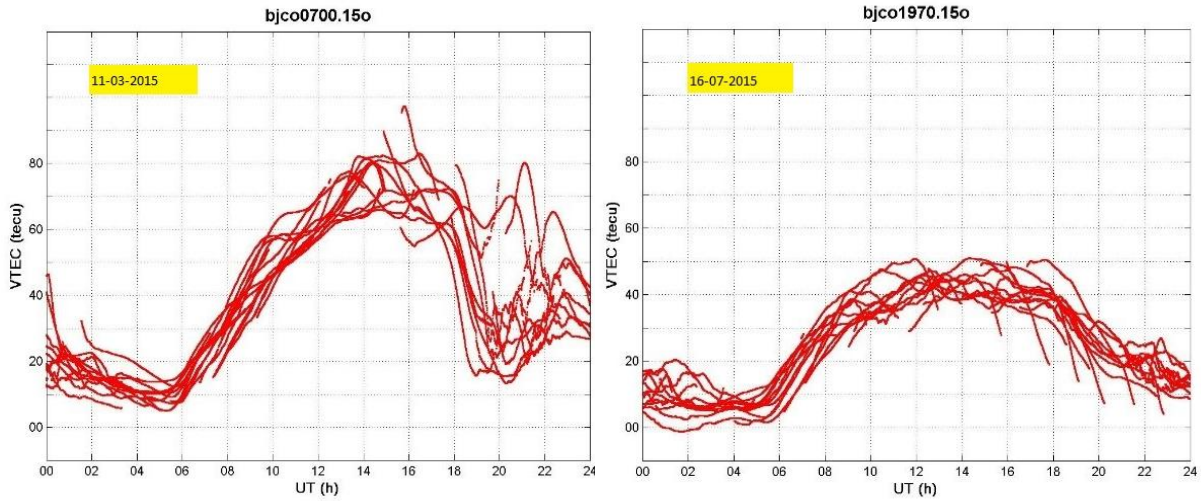


***Figure 4a*** ***Figure 4b***

*Plots of VTEC variation respectively for March 11th 2015 and July 16th 2015 of the Cotonou station (BJCO)*

On March 11th, 2015, we note a strong diurnal evolution of the vertical total electronic content (VTEC) profile with a minimum at the end of the night (~ 5TU) and a quick increase towards the maximum of 14-16h, again around 90 tecu. The Figures 2a, 2b, 3a, 3b, 4a and 4b show the similar variation at the 3 GPS stations (DAKR, YKRO, BJCO). We validate a weaker diurnal peak around 45 tecu for July 16, 2015.

The second observation concerns the period after 20 UT with a rise in TEC and above all a large range of variations in TEC between different satellites being tracked. This reflects the

presence of large spatial gradients of ionization. In addition, one can foresee fluctuations of smaller scales more numerous in Dakar than on the two other stations.

### 4.2. ROTI index Analysis

The ROTI index calculation described in section 2.2 allows it to be viewed as a function of time. We have plotted each value by the sign '+' in Figures 5a, 5b, 6a, 6b, 7a and 7b.

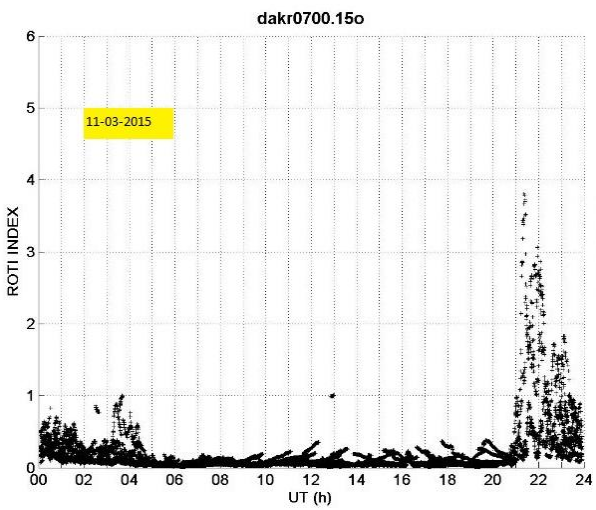


***Figure 5a***

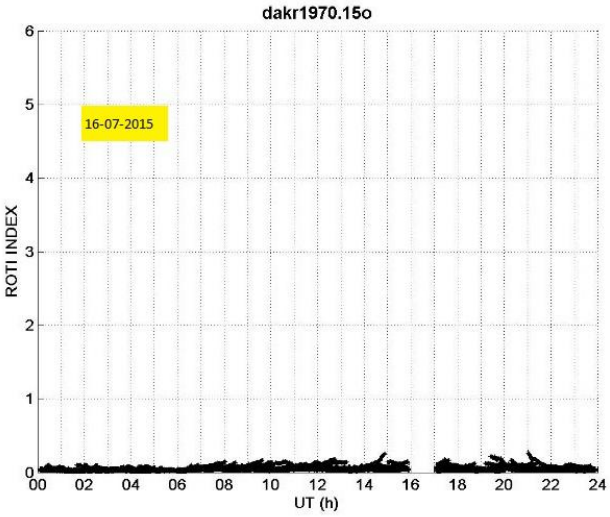


***Figure 5b***

*Plots of ROTI index variation respectively for March 11th 2015 and July 16th 2015 of the Dakar station (DAKR)*

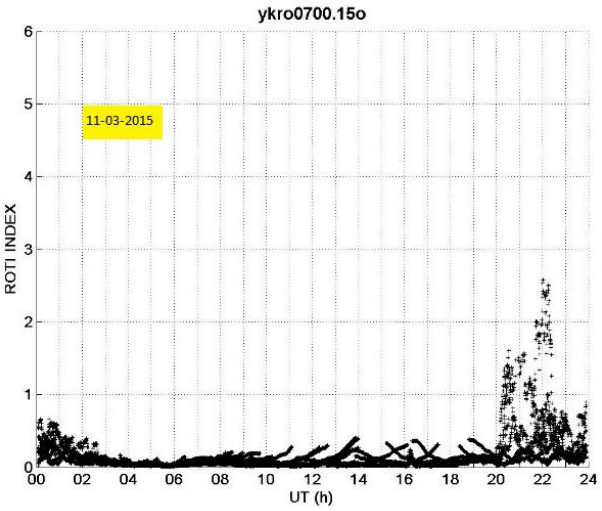


***Figure 6a***

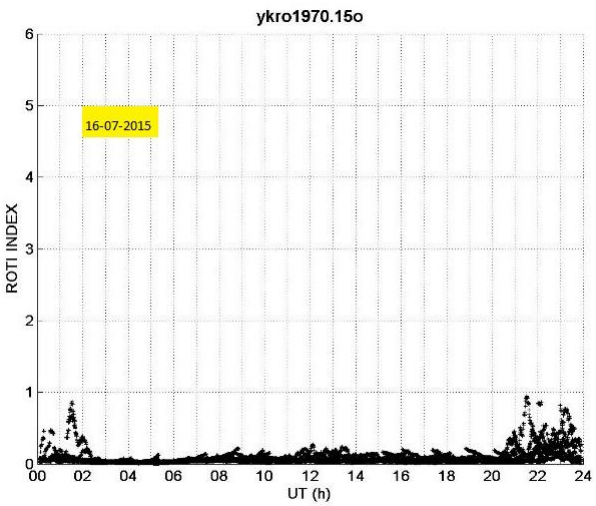


***Figure 6b***

*Plots of ROTI index variation respectively for March 11th 2015 and July 16th 2015 of the Yamoussoukro station (YKRO)*

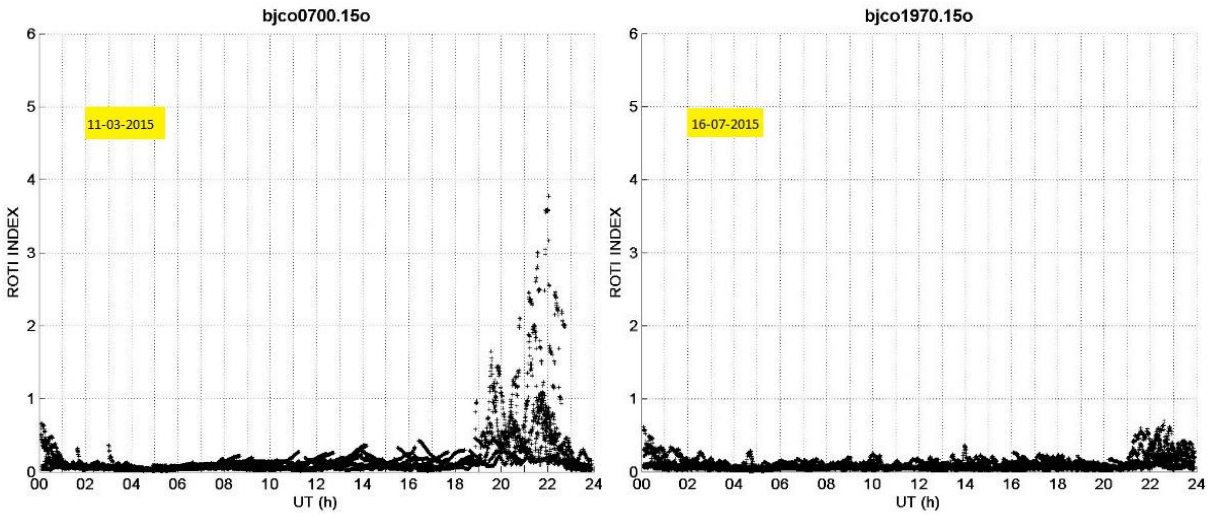


***Figure 7a*** ***Figure 7b***

*Plots of ROTI index variation respectively for March 11th 2015 and July 16th 2015 of the Cotonou station (BJCO)*

On March 11th, 2015, scintillation was observed from 8 p.m. local on the 3 stations and continued until midnight. It is high at the start of the period at DAKR and rather low at the end of the period at BJCO. The values are somewhat lower (<3 units) at YKRO.

The contrast is significant with July 16, 2015. In this case, there is no value above 1 tecu / min. We note only a weak rebound, not significant, over the period 8 p.m. to midnight for the YKRO station. This situation allows us to conclude that there is no scintillation on this particular day. These conclusions on the presence of strong scintillation at the equinoxes and its absence in summer on the 20h-24h TL time slot is consistent with previous publications **[3]** and **[15]**.

### 4.3. Positioning analysis

To calculate the position of the stations, we therefore used the RTKlib software because it allows dynamic positioning, that is to say, it makes the calculation at each measurement period from the phase measurements. As input, we have the same RINEX file used for the calculation of the ROTI index. The software also requires knowing the position of the GPS satellites obtained thanks to the ephemeris navigation files archived by the IGS network (Olwendo, 2018). The two correction models for the propagation parameters are the Saastamoinen model for the troposphere and the GIM / CODG maps for the ionosphere. We have also retained that the measurements above 15° of elevation because of the influence of the multipaths on the measurements. The software visualizes the 3 polar components of the position as a function of time which is the UTC time on the abscissa. The upper block is longitude in meters, the middle block represents latitude in meters, and the lower block is altitude also in meters. The scale in y is in all cases ± 50m.

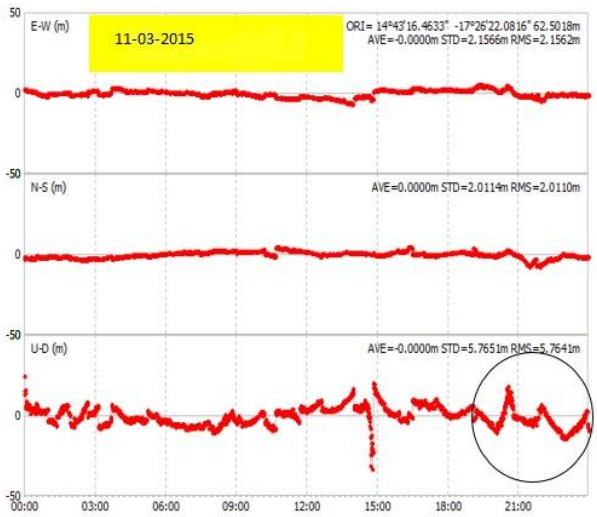


***Figure 8a***

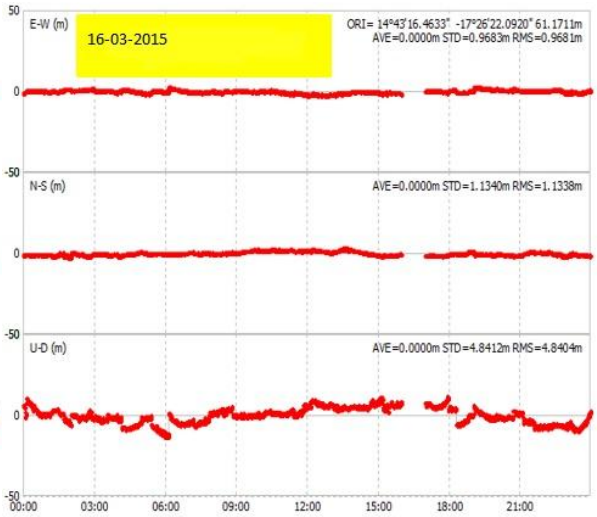


***Figure 8b***

*Positioning plots respectively for March 11th 2015 and July 16th 2015 for the Dakar station (DAKR)*

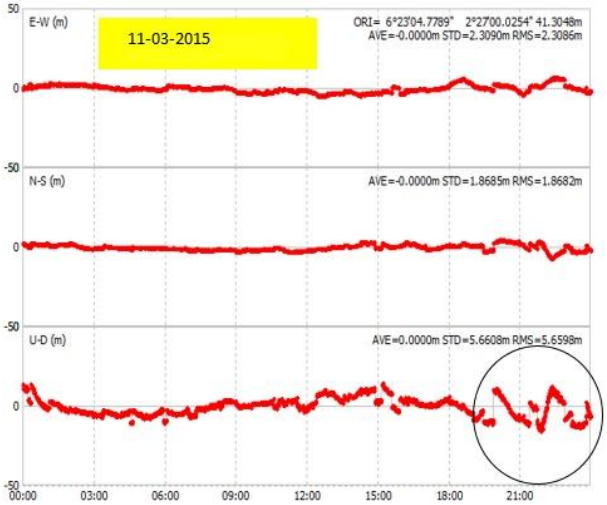


***Figure 9a***

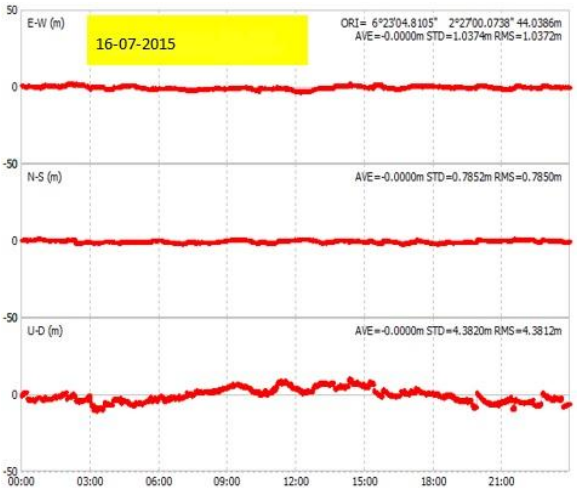


***Figure 9b***

*Positioning plots respectively for March 11th 2015 and July 16th 2015 of the Yamoussoukro station (YKRO)*

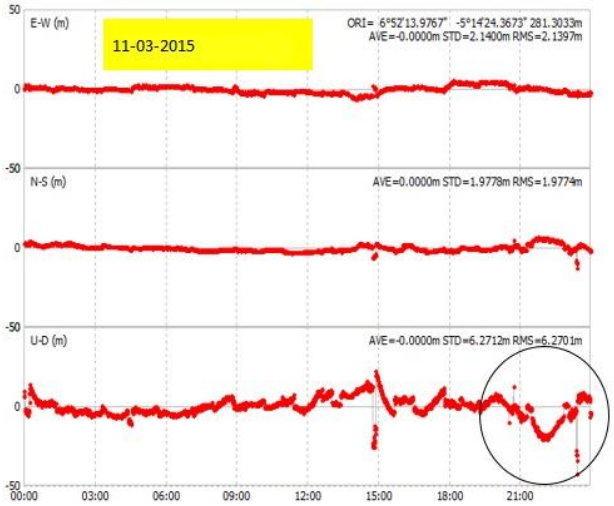


***Figure 9a***

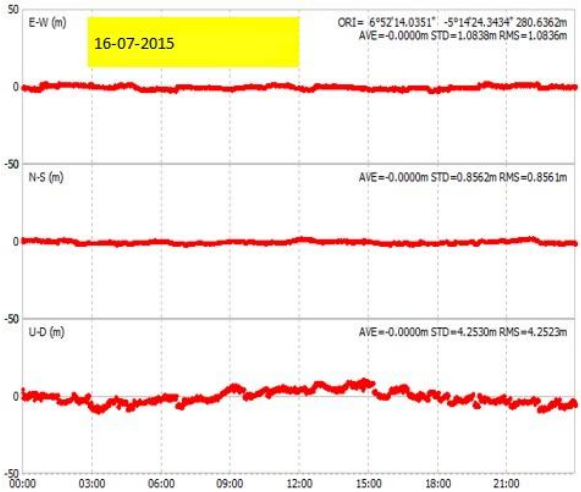


***Figure 9b***

*Positioning plots respectively for March 11th 2015 and July 16th 2015 of the Cotonou station (BJCO)*

The following Table2 gives average values of positioning errors of three (03) stations.

Table 2: Average values of positioning errors

| GPS marker | Latitude error deviation (m) | Longitude error deviation (m) | Altitude error deviation (m) |
|---|---|---|---|
| DAKR | 2.16 | 2.01 | 5.76 |
| BJCO | 2.14 | 1.98 | 6.27 |
| YKRO | 2.31 | 1.87 | 5.66 |

In the three (03) cases of stations, the deviation in latitude and longitude does not exceed a few meters (RMS error of 2.5m) and it is the altitude that presents the greatest variability with an RMS deviation between 5 and 6m. The largest deviations from the average are located on March 11th, at the end of the day, meaning that in the 20h-24hTU range as shown by the areas circled in black. This corresponds to the period with strong scintillation modeled by the ROTI index. In addition, the deviations are not present on the day of July 16th where we had already noted an absence of scintillation. We therefore have a typical degradation link in the determination of altitude in the presence of scintillation. Small disturbances of the phase measurements are visible on the suit for calculating. the TEC as well as quantifying the ROTI index and therefore causing lower precision in the altitude determination.

The correlation between the ROTI index and the altitude degradation at each moment of measurements is more difficult to observe. This can come from the geographical position calculation which is based on Kalman filtering and therefore which can take into account a numbers of measurements through the instantaneous calculation, we do not have the answer to this question.

## 5. Conclusion

In this work, we were able to observe the impact of ionospheric irregularities on GPS signal positioning. We have retained two typical situations, one with the presence of scintillation on GPS signal and the second without any scintillation. The latter was observed by calculating the ROTI index on TEC measurements. The RTKlib software allowed us to calculate the three positions in dynamic mode (PPP for "Precise Point Positioning") that is to say at each epoch of the measurement provided by the RINEX file. We observed a strong correlation between strong values of the ROTI index above 1 tecu / mn and a degradation in the calculation of the station altitude (which is fixed). Deviations of 25m were obtained from the mean trend. The other two components (latitude and longitude) are hardly impacted by the scintillation phenomenon. For future work, we propose to treat and analyze a broader base of scenarios and to try to establish a metric between the level of the ROTI index and altitude.

## 6. References


**[1]** P.L.N. Raju, Fundamentals of GPS, Geoinformatics Division, Indian Institute of Remote Sensing, Dehra Dun, Satellite Remote Sensing and GIS Applications in Agricultural Meteorology pp. 121-150.

**[2]** Davies, B., & Harré, R. (1990). Positioning: The discursive production of selves. Journal for the Theory of Social Behaviour, 20(1), 43–63

**[3]** Aarons J., Global morphology of ionospheric scintillation, Proc. IEEE, v70, p360-378, 1982.

**[4]** Kahindo Murumba B., A. Mukenga Bantu K., Fleury R., Tondozi Keto F., Zana Ndontoni A., Kakule Kaniki M., Amory-Mazaudier C., Groves K.. Contribution à l'étude de la scintillation ionosphérique équatoriale sur la crête sud de l'Afrique. Journal des Sciences I.S.S.N 0851 – 4631, 2017.

**[5]** Y. T. Chiu and J. M. Straus. Rayleigh-Taylor and Wind-Driven Instabilities of the Nighttime Equatorial Ionosphere. Journal of geophysical research VOL. 84, NO. A7 JULY, 1979)

**[6]** Kintner P.M., Ledvina B.M., De Paula E.R., GPS and ionospheric scintillations. Space weather, vol. 5, S09003, 2007.

**[7]** Olwendo, J., Cilliers, P., A comparison of ionospheric scintillation proxy indices derived from low rate IGS data with the amplitude scintillation index, S4, in a low latitude region over Africa, Journal of Atmospheric and Solar-Terrestrial Physics, https:// doi.org/10.1016/j.jastp.2018.04.012, 2018.

**[8]** Conker R.S., El-Arini M.B., Hegarty C.J., Hsiao T., Modeling the effects of ionospheric scintillation on GPS/satellite-based augmentation system availability. Radio Science, vol. 38, 1–23, 2003.

**[9]** Moreno B., Radicella S., De Lacy M.C., Herraiz M., Rodriguez-Caderot G., On the effects of the ionospheric disturbances on precise point positioning at equatorial latitudes, GPS Sol., v15, p381-390, 2011.

**[10]** Zhang X., Guo F., Zhou P., Improved precise point positioning in the presence of ionospheric scintillation, GPS sol., v18, p51-60, 2014.

**[11]** Zhenlong Fang, Wenfeng Nie, Tianhe Xu, Zhizhao Liu, and Shiwei Yu, Accuracy Assessment and Improvement of GNSS Precise Point Positioning Under Ionospheric Scintillation, J. Sun et al. (Eds.): CSNC 2019, LNEE 563, pp. 400–411, 2019. https://doi.org/10.1007/978-981-13-7759-4_36

**[12]** Acharya R., S. Majundar, Statistical relation of scintillation index S4 with ionospheric irregularity index ROTI over Indian equatorial region. Advances in Space Research Vol. 64, Issue 5, Pages 1019-1033, 2019.

**[13]** Basu S., Groves K.M., Quinn J.M., Doherty P., A comparison of TEC fluctuations and scintillations at Ascension Island, Journal of Atmospheric and Solar-Terrestrial Physics, v61, p1219-12226, 1999.

**[14]** Liu Y., Radicella S., On the correlation between ROTI and S4, Annales Geophysicae, 14p, https://doi.org/10.5194/angeo-2019-147, 2019

**[15]** Pi, X., Mannucci, A., Lindqwister, U., Ho, C., Monitoring of global ionospheric irregularities using the worldwide GPS network. Geophys. Res. Lett., v24 (18), 2283–2286, 1997.

**[16** Mulugeta, S., Kassa, T., Nighttime Ionospheric irregularities inferred from Rate of Total Electron Content Index (ROTI) values over Bahir Dar, Ethiopia, Advances in Space Research, 2020.

**[17]** Lassudrie Duchesne P., Béniguel Y., Bourdillon A., Fleury R., Valette J.J., et al. Les effets de la scintillation ionosphérique sur le GPS. Navigation, 58 (231), pp.17 – 34, 2010.

**[18]** Takasu T,, Yasuda A., RTKLIB ver. 2.4.2 Manual, 181p.

**[19]** Dubey S., Wahi R., Mingkhwan E., Gwal A.K.. Study of amplitude and phase scintillation at GPS frequency. Indian Journal of Radio & Space Physics, vol. 34, pp. 402-407, 2005.

**[20]** Leica Geosystems AG, Heerbrugg, Switzerland, 2017, 832702-3.0.0en.

**[21]** Guo, J., Dong, Z., Liu, Z., Mao, J. and Zhang, H. (2017) 'Study on ionosphere change over Shandong based from SDCORS in 2012', Geodesy and Geodynamics, 8(2017), pp. 229–237.

**[22]** Zoundi. C., Ouattara. F., Fleury. R., Amory-Mazaudier. C., Lassudrie Duchesne. P. Seasonal TEC Variability in West Africa Equatorial Anomaly Region. European Journal of Scientific Research ISSN 1450-216X, vol.77, pp.309-319, 2012.